aerospace

MDPI

Article

Design and Structural Analysis of a Control Moment Gyroscope (CMG) Actuator for CubeSats

Alexis Gaude and Vaios Lappas *

Centre for Cyberphysical and Autonomous Systems, School of Aerospace, Transport and Manufacturing, Cranfield University, Bedford MK43 0AL, UK; a.gaude@cranfield.ac.uk

* Correspondence: vlappas@cranfield.ac.uk

Received: 15 April 2020; Accepted: 6 May 2020; Published: 11 May 2020

Abstract: Following a global trend towards miniaturization, the population of nano- and micro-satellite continues to increase. CubeSats are standardized small size satellites based on $10 \times 10 \times 10$ cm cube modules (1U) and are becoming sophisticated platforms despite their very small size. This paper details the design and the structural analysis of a Control Moment Gyroscope (CMG) actuator for agile CubeSats with a physical size up to 12U, which require high torque actuators. CMGs have inherited torque amplification capabilities and the recent advances in motor miniaturization make them ideal candidates for small satellite missions with slew rate requirements. The system's requirements are derived based on conceptual agility requirements for an agile (highly maneuverable) CubeSat which needs to achieve a 90° maneuver in 90 s. With specific cost, mass and volume requirements, the proposed CMG design is based on some of the smallest available off-the-shelf electric motors and uses a light aluminum casing design. The proposed design uses stepper motors for the gimbal mechanism as a low cost, compact and low power solution, contributing to an overall low mass of the full CMG cluster. Static and dynamic analyses were performed to assess the mechanical integrity of the system for launch loads. Apart from a necessary custom control electronic board, the complete mechanical assembly has been designed including electrical hardware. Analyses demonstrate that the overall stress levels acting on the system are manageable by the CMG design. Bolted joints are critical and should be studied independently as the chosen model created singularities around these areas. Each individual CMG of the designed pyramidal cluster is shown to weigh about 35 g. Using the proposed CMG design with a customized avionics board, the complete CMG system is shown to weigh 250 g and occupies slightly more than $\frac{1}{2}$U volume for a CubeSat, indicating the feasibility of CMGs for agile CubeSats.

Keywords: CubeSat; attitude control; control moment gyroscope; finite element analysis

1. Introduction

Since the third industrial revolution, the miniaturization trend of vehicle systems has grown substantially. The miniaturization of such systems described by the famous Moore's law, has not only applied in the field of electronics, but has also been applied in many industrial fields such as space systems. As such, the satellite market is not excluded from this trend and in the last few decades, the number of nano- and micro-satellites has been increasing and it has been shown in multiple forecast studies that this trend is likely to continue [1].

In April 2019, the European Space Agency (ESA) created a unit dedicated to CubeSats [2], highlighting the importance of standardized nanosatellites and their growing market share in the space market. Developed in 1999 by the California Polytechnic State University and Stanford University, CubeSats are specified, standardized small-size satellites initially designed for education and now used for commercial and scientific missions. They were designed with standard interfaces and dimensions

based on a 10 × 10 × 10 cm (referred to as 1U blocks/units) form factor CubeSats with form factors of 6, 9, 12 and 16U are now being studied and manufactured for multiple institutional and commercial earth observation, space science/exploration and technology demonstration missions

Miniaturization of a satellite implies miniaturization of all its components. Although small satellite development and the growth in the performance and capabilities of these systems is mostly attributed to the advent of microelectronics, improvements in micro motors, mechatronics and sensors has enabled the design of miniature momentum exchange devices for advanced high precision three-axis stabilized CubeSats [3–5]. Momentum wheels and reaction wheels are now common actuators on CubeSats and, although they do offer adequate attitude control capabilities, the power, volume and mass constraints of CubeSats limit the angular momentum and torque performance of these technologies. Higher levels of agility, with higher slew rates (>0.5 deg/s) allow satellites to take more images per orbit due to their increased maneuverability [6–9]. The ability to capture more images by being more maneuverable is a key feature of many recent earth observation satellites, such as Pleiades, WorldView-3 and -4, as more images translates to an increase in the commercial value of the satellite and the overall mission. Agile satellites with high slew rates require high toque and angular momentum systems such as Control Moment Gyroscopes (CMG) [6–12]. CMGs are momentum wheels gimballed in one or two axes, amplifying and generating torque by gimballing a momentum wheel spinning at a constant speed which is storing angular momentum. CMGs were previously used in larger satellites, however, miniaturized versions have flown on medium-sized satellites (Pleiades, Worldview-3/4) as well as small satellites [6,11,12]. In this paper, the focus is set on designing a Control Moment Gyroscopes actuator (CMG) as part of an attitude control subsystem for CubeSats with a high agility (maneuverability) requirement. A nano-CMG is designed for a 3U CubeSat platform and a preliminary structural analysis is presented which indicates that a small CMG cluster can be feasible and can fit in a 1U volume for a CubeSat mission with high agility (>1 deg/s) requirements.

1.1. CMG Dynamics

A CMG uses a flywheel that has a high rotating rate around its axis and can rotate around one or more of its perpendicular axes called gimbal axes. The change in angular momentum creates a torque $\underline{T}$ perpendicular to both the spin direction—direction of the angular momentum $\underline{h}$—and the angular velocity of the gimbal $\underline{\delta}$ [3,6,7,9,10]. Its value is given by Equation (1).

$$\underline{T} = \underline{h} = \underline{\delta} \times \underline{h} \tag{1}$$

A CMG with one gimbal axis is called a Single Gimbal CMG (SGCMG), one with two gimbal axes is called a Dual Gimbal CMG (DGCMG). At least three SGCMG are necessary for three-axis attitude control. But if two CMG's spin axes were to become parallel due to a configuration of the gimbal angles, one of the degrees of freedom would be lost. This is called singularity and can be avoided using control laws and specially designed clusters [4–10] such as:

- Six parallel mounted SGCMGs, used in Mir (1986–2001);
- Three orthogonally mounted DGCMGs, used in Skylab (1973–1979);
- Four parallel mounted DGCMGs, used in the International Space Station (1998–);
- A pyramid configuration of four SGCMGs.

The latter, a 4-SGCMGs pyramidal configuration, has been proposed and used for multiple large and small satellite applications and is well described in the literature [4–9]. The 4-SGCMG cluster at an angle of 54.7° is used in our analysis and is the most common configuration used for CMG-equipped satellites as it can produce the same angular momentum in every direction. Figure 1 illustrates the classical CMG cluster configuration.

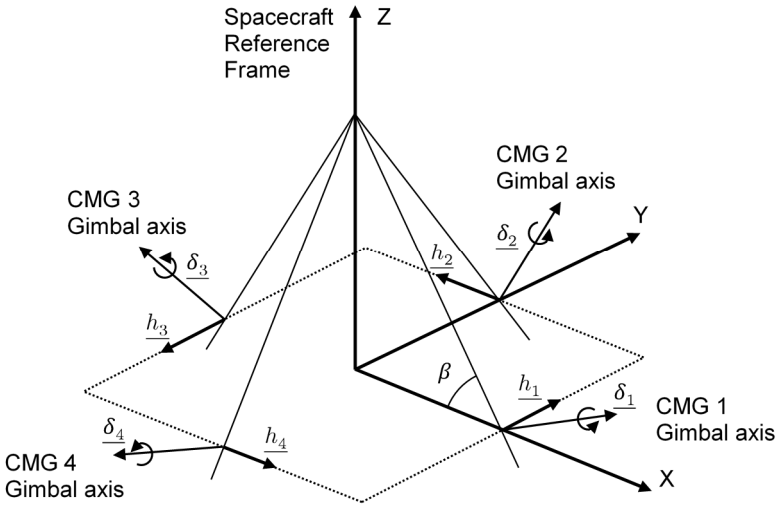

Figure 1. 4-SGCMGs Pyramid Configuration [6,7].

Equation (2) details the total angular momentum of the cluster in the spacecraft reference frame.

$$\begin{aligned} \underline{h} &= \sum_{i=1}^{4} \underline{h_i}(\delta_i) \\ &= h_1 \begin{bmatrix} -cos\beta sin\delta_1 \\ cos\delta_1 \\ sin\beta sin\delta_1 \end{bmatrix} + h_2 \begin{bmatrix} -cos\delta_2 \\ -cos\beta sin\delta_2 \\ sin\beta sin\delta_2 \end{bmatrix} + h_3 \begin{bmatrix} cos\beta sin\delta_3 \\ -cos\delta_3 \\ sin\beta sin\delta_3 \end{bmatrix} \\ &+ h_4 \begin{bmatrix} cos\delta_4 \\ cos\beta sin\delta_4 \\ sin\beta sin\delta_4 \end{bmatrix} \end{aligned} \tag{2}$$

With h_i, the magnitude of the angular moment of each SGCMG. While the gimbal angles δ_i will change over time, the skew angle β is a fixed geometric parameter of the cluster. This angle is often taken as $\beta = 54.73$. Considering all CMGs' angular momentum equal—in fact, CMGs are often identical—the momentum envelope of a 4-SGCMGs Pyramid Configuration with a skew angle of 54.73° is nearly spherical. That is, the total angular momentum of the cluster is almost equal in any direction (for any configuration of gimbal angles).

A spacecraft follows Euler's equation of motion that dictates its attitude [6,7]. In the spacecraft reference frame, Equation (3) describes the change in angular momentum $\underline{H}$ with respect to an applied external torque $\underline{T_{ext}}$ and the spacecraft rotation rate $\underline{\omega}$.

$$\underline{H} = \underline{T_{ext}} - \underline{\omega} \times \underline{H} \tag{3}$$

The angular momentum considered here is that of the whole spacecraft including rotating subsystem (e.g., CMGs) and thus can be divided in Equation (4) into the sum of the product of the spacecraft moment of inertia $\underline{\underline{J}}$ with the spacecraft rotation rate $\underline{\omega}$ and the total angular momentum of the CMG cluster $\underline{h}$.

$$\underline{H} = \underline{\underline{J}}\,\underline{\omega} + \underline{h} \tag{4}$$

Equation (5) introduces the rate of change of the spacecraft angular velocity deriving Equation (4).

$$\underline{H} = \underline{\underline{J}}\,\underline{\omega} + \underline{\underline{J}}\,\underline{\omega} + \underline{h} \tag{5}$$

which gives Equation (6) inserting Equation (3).

$$\underline{\underline{J}}\,\underline{\dot{\omega}} + \underline{\omega} \times \underline{\underline{J}}\,\underline{\omega} = \underline{T_{ext}} - \underline{\dot{h}} - \underline{\omega} \times \underline{h} - \underline{\underline{J}}\,\underline{\dot{\omega}} \quad (6)$$

1.2. Small Satellite CMG Hardware

As mentioned before, the advent of microelectronics, sensors, materials and micro-motors has made CubeSats to become versatile and capable platforms for a range of missions including Earth observation. As CubeSats are becoming more advanced, agility has become an area of growing interest for these small satellites. As agility requires high torque actuators, there are a number of miniature CMG developments for ground experiments and for future flight missions. Table 1 summarises some of the most recent and relevant CMG designs proposed for small satellites. In Table 1, the SwampSat, Tsubame, Lappas, Baker and Cranfield CMGs parameters refer to 4-CMG clusters. The Honeybee CMG is available in multiple configurations and is presented as a single unit and BILSAT-1 used a 2-CMG parallel arrangement [6–19].

Table 1. Existing CMGs for small satellites.

Parameter	SwampSat [1] [16]	Honeybee [2] [17]	Tsubame [2] [18]	Lappas [6,12]	Baker [19]	BILSAT-1 [3] [11]	Cranfield CMG
Size [mm]	100 × 100 × 50	48 × 48 × 91	Ø50 × 134	150 × 150 × 50	96 × 96 × 96	135 × 155 × 190	100 × 100 × 50
Mass [kg]	0.437	0.6	0.960	1.170	842	2.2	0.250
Peak power [W]	3.2	2	4	2	N/A	12	2.5
Maximum torque [mN·m]	0.8	172	31	52.25	1.4	55.9	1
Angular momentum [mN·m·s]	0.8	86	52.7	1000	4.5	280	0.629
Gimbal rate [rad/s]	1	N/A	1	0.2	10	0.1	1

[1] Iteration 2, [2] CMG Unit, [3] Cluster with 2 CMGs.

The first CMG development for small satellites involved a 52.25 mN·m CMG in a classical CMG cluster which was successfully demonstrated using a ground-based air bearing system to simulate satellite attitude motion. The CMG test validated the performance, mass and power benefits of CMGs for small satellite missions with a high slew rate requirement. The use of low-cost Commercial Off-The-Shelf (COTS) Direct Current (DC) motors for the flywheel and of miniature stepper motors for the gimbal motor showed that low power CMGs can be a viable and useful option for small satellites [6,12].

SwampSat was a 1U-CubeSat student mission developed by the University of Florida in Gainesville, FL, USA and included a 4-CMG payload. The Purpose of the satellite is to demonstrate quick and accurate ACS using CMGs on pico-satellite [16]. The CMG used in SwampSat is one of the few designed to be used in a nanosatellite as its size is only half a CubeSat unit. The CMG uses a double-ended brushless DC motor with two identical flywheels on both sides. The advantage of using two flywheels is to reduce the size of each flywheel, gaining in equilibrium, allowing for higher inertia, and reducing the cantilevered issue of having a heavy flywheel on one side of the motor, while also making the overall CMG volume more compact in order to fit in a 1/2 U volume, which is why the CMG skew angle was set to 30°. Launched in 2013, the satellite was not able to transmit or received any commands due to technical issues.

Honeybee Robotics' Microsat Control Moment Gyroscope is a SGCMG that can be used in any cluster configuration the user should choose. They claim to have a CubeSat compatible option [17] in a 90° box array configuration. The size of the cluster would be 230 × 125 × 82 mm (including electronics) for a total power consumption of 10 W (peak) [17]. The Honeybee CMGs were designed for 23 kg-sized microsatellites with an acceleration requirement of 3 deg/s^2 and designed to fit 1U.

Similar to the CMG developed in Ref. [6,20] and SwampSat [15,16], Baker [19] developed a miniature CMG for a 16U (CubeSat form factor [20,21]), 38-kg satellite with a 3 deg/s slew requirement.

The proposed CMG design involved the use of a stepper motor for the gimbal as in Ref [6] due to the low power and mass advantages, and was shown to be a viable option for microsatellites with a CMG cluster mass less than 1 kg, as shown in Table 1. Tsubame's CMGs, developed for a 49-kg microsatellite, used hysteresis synchronous motors for the flywheel and hybrid-type stepper motors for the gimbal [18]. Using AC motors generally reduces power consumption compared to DC motors but result in a loss in speed control. A stepper motor for the gimbal was selected to allow for easy and precise control of the gimbal angle, controlling the motor step-by-step (a fraction of angle). A Hybrid stepper is more expensive and heavier (but the added mass, compared to a permanent or variable reluctant stepper, is on the rotor thus increasing the inertia of the flywheel). But it has smaller steps, higher step rate and a higher torque. The CMG used a very high flywheel speed, above 20,000 rpm. The satellite launched in 2014 but encountered technical problems and was never commissioned.

Based on the work of Lappas et al. [6,12], a twin CMG experimental payload funded by TUBITAK (Turkey) and ESA was developed for the 120 kg BILSAT-1 microsatellite [22]. The CMG used a Faulhaber DC brushless motor for the flywheel and is gimbaled with a stepper motor. This choice is justified by several advantages of stepper motors (low power) over DC motor: "simplicity, robustness and ease of control for low speeds". The Commercial Off-The-Shelf (COTS) stepper was modified to survive the space environment. This model has the particularity to only allow a ±180° rotation about its neutral position. The CMGs were tested successfully in the BILSAT-1 small satellite and are the only small satellite CMGs flown in orbit to date.

In summary, CMGs, whether there are used for large satellites or for small, can bring significant mass, performance and volume savings/benefits compared to traditional reaction wheel systems. The inherit torque amplification effect of CMGs due to the momentum stored in the CMG flywheel combined with the use of low cost, low power stepper motors for the gimbal mechanism make the CMG an elegant and advantageous actuator, even for CubeSat-sized platforms where volume and mass is even more critical than in larger sized platforms. A detailed analysis on the torque, mass and power benefits of miniature CMGs compared to reaction wheels has been presented in [6,12], which proved CMGs to be a low cost, viable option for small satellites.

2. CMG Objective and Requirements

The objective is to design and verify the mechanical integrity a 4-SGCMG pyramid cluster for a 1 to 12U CubeSat. The system should be designed to be as compact and light as possible while remaining at a reasonable cost. Thus, only Commercial Off-The-Shelf (COTS) hardware is to be used. The system is not to be designed for a specific mission; thus, it should be modular to fulfil the need of various missions. The CMG should comply with the following requirements (used for the SwampSat CMG): A maximum mass of 500 g, a maximum volume of $\frac{1}{2}$ CubeSat-Unit (100 × 100 × 50 mm) and a maximum power of 3 W. It is required that the CMG must allow the satellite to rotate 90° in 90 s. An average slew rate of 1 deg/s is used based on recent earth observation satellite missions [6,8,9,13].

Assuming a 12U-CubeSat as a 240 × 230 × 360 (x × y × z) mm [21] homogeneous cuboid of 12 kg, the principal moment of inertia of the satellite can be computed. For the 12 kg 12U CubeSat, the inertia is: $\underline{\underline{J}} = \begin{bmatrix} 182500 & 0 & 0 \\ 0 & 187200 & 0 \\ 0 & 0 & 110500 \end{bmatrix} \text{kg} \cdot \text{mm}^2$

From Equation (6), assuming a non-rotating satellite (i.e., $\omega = 0$) and no external torque, Equation (7) gives the minimum absolute value of the torque that the CMG must create for a given angular acceleration.

$$\underline{\underline{J}}\,\underline{\omega} = -\underline{h} = -\underline{T} \tag{7}$$

The spacecraft acceleration is computed since that the fastest way to rotate 90° in 90 s is to have a constant positive acceleration for half the time and a constant negative acceleration for the second

half. Then, from Equation (7), for the worst case (i.e., a rotation around the y axis), the derived torque requirement is computed to 0.145 mN·m.

For a single-axis rotation around the Y-axis, only the two CMGs aligned with the Y-axis are used. The torque produce by those two CMGs must be oriented such as the z components cancel each other, and the y components add each other. Thus, the total torque acting on the satellite provided by CMG #2 and #4 (indentation from Figure 1) is given by Equation (8) below [6]:

$$\underline{T} = 2h_0\delta cos\beta cos\delta \tag{8}$$

assuming the CMGs have the same momentum and their motion is symmetrical, hence $h_0 = h_2 = h_4$ and $\delta = \delta_2 = \delta_4$. The gimbal rate is taken equal to 0.2 rad/s, δ = 0 and β = 54.73°. The minimum momentum for each CMG is 0.629 mN·m·s.

Considering that the gimbal angle must be known with an error less or equal to 0.1°, the requirements are summarized in Table 2. The CMG parameters are used as the driving requirements; however, the hardware selection allows for an increase in torque and angular momentum performance due to the possibility to increase the flywheel speed and gimbal rate (higher than 1 rad/s).

Table 2. CMG requirements.

Parameter	Value	Condition
Mass	500 g	Maximum
Volume	$\frac{1}{2}$ CubeSat-Unit (100 × 100 × 50 mm)	Maximum
Power	3 W	Maximum
Torque (cluster)	0.145 mN·m	Minimum
Angular momentum (CMG)	0.629 mN·m·s	Minimum
Gimbal angle error	0.1°	Maximum

3. CMG Design

The main components of a CMG consist of:

- A flywheel and its motor used to create the angular momentum.
- A second motor—the gimbal motor with a gearhead—rotates the whole flywheel assembly, made up of the first two pieces of hardware and a bracket, creating torque.
- One or several bearings to guide the rotation and to prevent the gimbal motor or gearhead to withstand any bending moment during launch.
- A position sensor that might be necessary to provide accurate initial position of the system once in orbit.
- Finally, a slip ring allowing current and information coming from the rotating flywheel assembly to be routed to controllers.

Some designers might want to replace the need of a slip ring by preventing, via a software logic, the flywheel assembly to rotate more than one full turn, or to reduce the system complexity; hence, two versions of the CMG have been designed with and without the slip ring.

The driving components of a CMG are the flywheel and the geared gimbal motors. The first determines the rate at which the flywheel rotates and hence the mass and size of the flywheel can be determined from the inertia requirements. The overall size (especially length) of the CMG is driven by the gimbal motor (especially the gearhead). The purpose of the flywheel motor is to maintain a high constant speed for the flywheel. For high speed purposes, the obvious choice is a DC motor. A stepper motor would jitter, and continuous servos typically do not have high rotation rates. Using a brushed DC motor is not possible as friction would make the brushes wear out and replacement is not possible in orbit. It would also increase power consumption. Thus, the only type of motor suitable for the flywheel is a brushless DC motor (BLDC motor)—it is the type of motor used in all the CMGs described in Section 1.2.

The driving characteristic of the gimbal motor is its precision. The angular rate and the angle swept must be accurately controlled. But the speed requirement is not excessive—it is fixed at 0.2 rad/s. Using a DC motor for the gimbal as in large CMG designs, or as in [16], can be problematic as it cannot easily be controlled with respect to position and, as the as the angular rate for the gimbal is low, a brushed DC motor with an absolute encoder can be a reasonable possibility but with a potential cost in mass and complexity. Using an absolute encoder would also ensure a precise initial position and consequently remove the need of a position sensor. A stepper motor, on the other hand, simply needs a fairly controller board as, once the initial angle is known, speed and angle can be precisely regulated with the step rate. As the gimbal rate requirement is relatively low (<1 rad/s), a stepper motor can be potentially the best choice from a power perspective and with multiple low cost, miniature models available. Considering the complexity, cost, and mass of the electronics required for a DC to control the gimbal position, a stepper motor was chosen.

Figure 2 shows an exploded view of the proposed CMG. COTS components are represented in dark grey, fasteners and other are in light grey (including bearings), manufactured parts of the gimbal assembly are in blue, and those of the flywheel assembly in red. Figure 3 shows the bearings configuration with and without the slip ring.

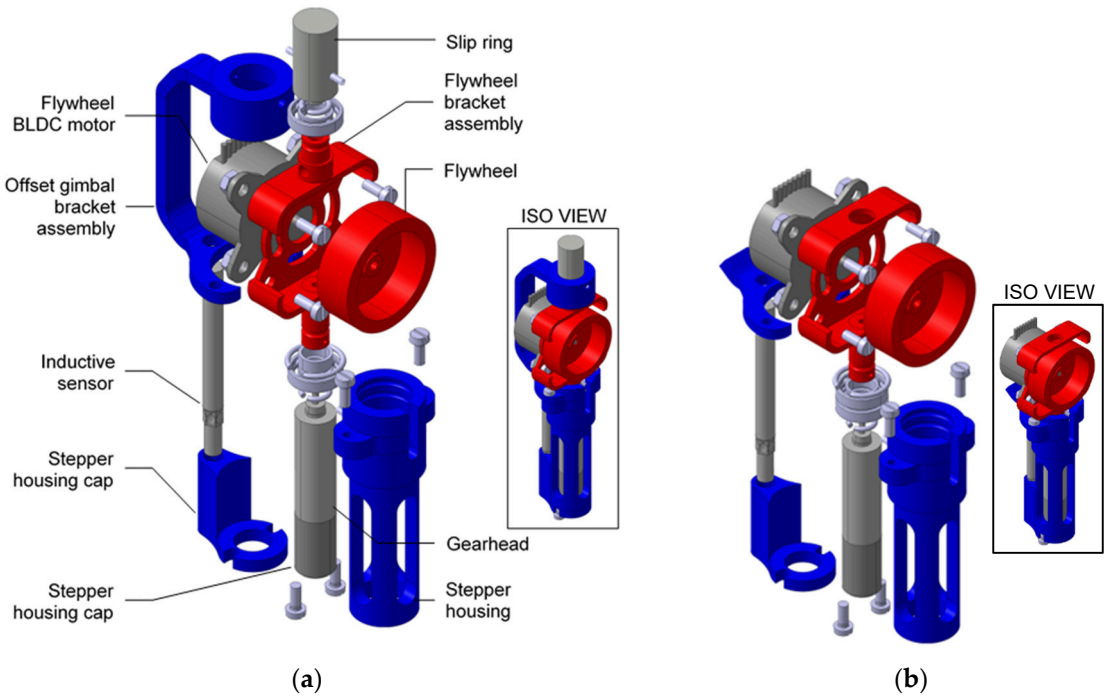

Figure 2. (**a**) CMG exploded and iso view with slip ring; (**b**) CMG exploded and iso view without slip ring.

The mass of a single CMG with slip ring is estimated at 35.065 g. Without the slip ring, the mass is estimated at 27.489 g. For a full system, four times this mass and the mass of the electronics must be considered for the full system mass. It is safe to assume that the electronics would weigh less than 359.74 g = 500 − (4 × 35.065). A standard CubeSat interface board is used, as the CMG avionics based on existing electronics means that the mass of board can be less than 80 g [4].

Manufactured parts that ensure the structural integrity of the CMG, position, and hold the COTS elements in place are made of aluminum AA 6061-T6 which is a standard grade for lightweight space rated applications. The flywheel is made of stainless steel from the AISI 300 grade as it would either be too light and its moment inertia too low, or too large if it were to be made in aluminum. All parts are designed to be manufactured with a lathe and/or a milling machine. Furthermore, a key requirement of the CMG design was to keep the costs of the unit low. The cost of the motors selected and assessed

were less than 200 EUR per motor as they are COTS technologies. The total cost of the motors, sensors and materials was estimated to be less than 500 EUR, with space-grade versions of the motors available from Faulhaber via customization.

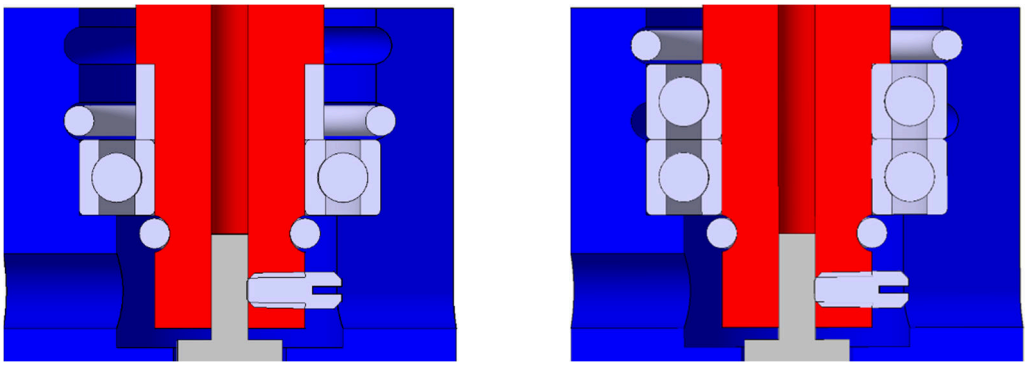

(**a**) (**b**)

Figure 3. Bearings configuration. (**a**) One bearing is above the flywheel on the slip ring housing, one is below the flywheel where a spacer and snap rings are used for shouldering; (**b**) Both bearings are placed side to side below the flywheel, the spacer is removed (replaced by the second bearing) and the internal snap ring move on the higher groove.

For the pyramidal cluster to work as intended, only the skew angled with respect to the CubeSat's reference frame and a 90° rotation between each CMG are necessary. Therefore, several dispositions are available, two interesting configurations are presented in Figure 4.

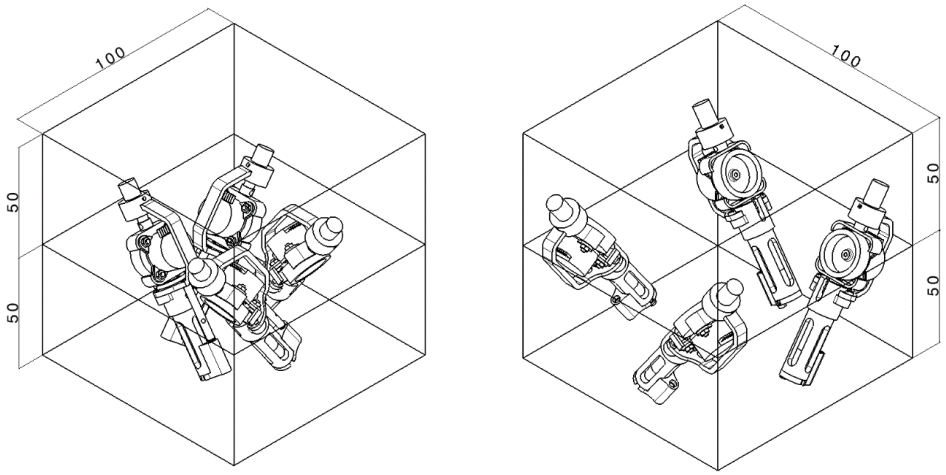

(**a**) (**b**)

Figure 4. Isometric view of two possible arrangement for the pyramid cluster. In wireframe, the outline of a standard 1U CubeSat with a separation at $\frac{1}{2}$U is represented. (**a**) Inside configuration, most compact possible and aims at reducing the volume occupied by the system to a minimum; (**b**) Outside configuration, less optimized in terms of compactness but is closer to the edges of the CubeSat making it easier to fix to the satellite. It also leaves the center free where a long and narrow payload or subsystem could fit (e.g., a telescope or a thruster).

The CMGs are quite tall—too tall to comply with the $\frac{1}{2}$U size requirement by 15 mm—yet very thin and some components can be fitted in the cluster's allocated $\frac{1}{2}$U, either around the CMGs in the 'inside' configuration or in between the CMGs in the 'outside' configuration, as shown in Figure 4. Obviously, some space must be saved for the control electronics. In both configurations, CMGs can be

rotated around their gimbal axis in order to position the offset gimbal bracket in such a way that it can be bolted onto an internal structure that would link the CMGs to the CubeSat. The no-slip ring version is smaller but does not comply with the size requirement either. However, from a volumetric point of view, the proposed CMG fits comfortably in the required $\frac{1}{2}$U volume.

4. Preliminary CMG Structural Analysis

Several Finite Element Analyses (FEA) were performed using ANSYS Mechanical (academic Version 19.1, Ansys Inc., Canonsburg, PA, USA) to check whether the CMG system would survive a launch and comply with launcher requirements. As the chosen launcher was not yet defined, the launch environment and requirements are derived from an ESA's Vega C as a realistic and representative example.

4.1. CMG Preliminary Analysis

First, a response spectrum analysis of an isolated flywheel assembly is performed as a preliminary step for a complete CMG analysis. In order to have an accurate model of the CMG it is important to find whether the flywheel assembly might rotate during the launch—acting as a revolute joint—or could be considered as a rigid link. A modal analysis is a prerequisite of a response spectrum analysis and was first performed.

The flywheel assembly considered for this analysis includes the flywheel, the flywheel bracket assembly, the BLDC motor, and the slip ring in the relevant case. The flywheel motor mount is bonded to the slip ring shaft, the gimbal shaft and the flywheel motor (a Brushless DC motor or BLDC). Two spherical joints are created between the ground and the upper and lower bearing seats. A revolute joint is defined between the rotor part of the slip ring and the slip ring shaft. The flywheel is bounded to the shaft of the BLDC and considered rigid. It would be able to rotate for a real launch, as there is no gear head on the BLDC, but it is not going to affect the torque on the gimbal axis much. The external surface of the slip ring and the inner surface of the gimbal shaft are fixed supports.

For the no slip ring version, the slip ring and the slip ring shaft are removed. All joints are the same, except the two spherical joints with the ground, replaced by only one revolute joint between the ground and the lower bearing seat. Indeed, alone, a bearing should be considered as a revolute joint for its play in bending, but the two side-to-side bearings in the no slip ring version cancel that play and can be modelled as a revolute joint.

The mesh is made of tetrahedron elements with a general size of 0.5 mm applied on all the components. Quadratic shape functions are used as it generally makes convergence faster (see later).

The base excitation is defined with an excitation in acceleration using Vega C's sine-equivalent vibrations [22] for a single launch configuration. The simulation's global coordinate system is defined in Figure 5.

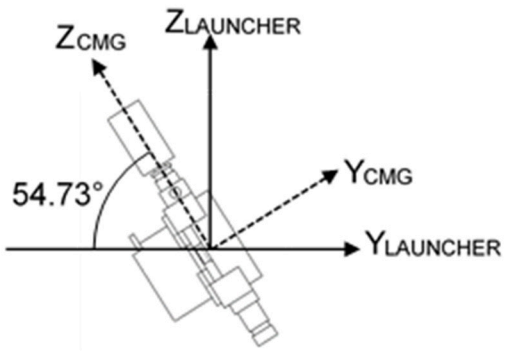

Figure 5. Simulation's coordinate system. The Z axis is the gimbal axis, the Y axis is the flywheel axis, and the X axis complete the right-hand rule.

Acceleration values are thus projected to take into account the skew angle. The CMG is rotated around the X axis, longitudinal accelerations are applied on the launcher's Z axis and lateral accelerations to the launcher's X axis. Values of the accelerations are displayed in Table 3.

Table 3. Sine acceleration projected onto the simulation's coordinate axis.

			X_{CMG}			
Frequency [Hz]	1	4.99	5	29.99	30	110
Acceleration [m/s^2]	3.924	3.924	7.848	7.848	4.905	4.905
			Y_{CMG}			
Frequency [Hz]	1	4.99	5	34.99	35	110
Acceleration [m/s^2]	2.227	2.227	4.531	4.531	5.664	5.664
			Z_{CMG}			
Frequency [Hz]	1	4.99	5	34.99	35	110
Acceleration [m/s^2]	3.203	3.203	6.407	6.407	8.009	8.009

A moment reaction probe computes the sum of the nodal moments expressed at the centroid of a boundary condition's support. Selecting the gimbal axis inner surface fixed support, the moment reaction probe returns the moment at the centre of the gimbal axis. The simulation's global coordinate system needs to be defined as it is because results are given projected onto these axes. Therefore, the results on the Z axis gives the reaction moment around the CMG's Z axis—which is the moment that the gearhead's axis would bear.

A mesh convergence of the gimbal shaft inner surface has been done to ensure the results are close to reality. Indeed, the smaller the mesh size, the closer the discretised finite element model is to the continuous reality. The mesh size cannot be reduced indefinitely, and practically, calculation time increases a lot with the number of elements. There is a point when the gain in precision due to mesh size reduction becomes insignificant compared to the increase in computation time. That is why mesh convergence is performed, to find the mesh size from which decreasing the mesh even more would have a small influence on the accuracy of the results. Results for various meshes are represented in Figure 6. The mesh of the inner surface of the gimbal shaft is refined from 0.5 to 0.1 mm with 0.1 mm increments.

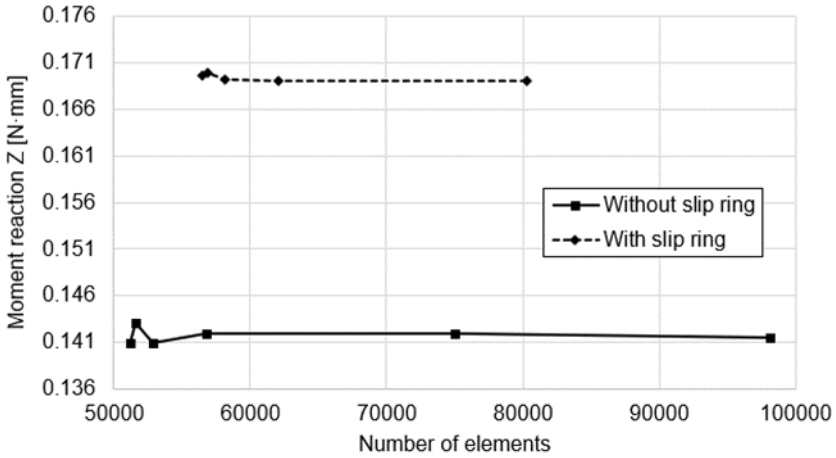

Figure 6. Moment reaction on the Z axis of the gimbal shaft fixed inner surface.

Results converge when the number of elements increases—mesh size decreases—meaning the results are not so mesh-dependant and close to reality. A greater moment is expected for the version with a slip ring. This is predictable as the inertia of the flywheel assembly is greater with a slip ring. The stepper residual torque (stepper's holding torque when not powered, a consequence of

the permanent magnets) has a value of 0.06 N·mm. With a 256:1 gear head ratio, that means the stepper will not rotate unless a torque greater than 15.36 N·mm is applied on the gear head. This is much greater than the 0.169 N·mm predicted by the analysis. This implies that during the launch, the flywheel assembly will not rotate around the gimbal axis. Although the position sensor becomes unnecessary, it is still included in the design in order to provide the option for potential utilisation.

4.2. Complete CMG Analysis

The CAD model of the CMG is modified for the analysis, simplifying some unnecessary features of the design. The following changes are applied:

- Threaded holes are converted into non-threaded holes whose diameters are the nominal diameters;
- The hexagonal shape of the sensor is simplified;
- Bearings, grub screws, snap rings and the spacer are removed.

The following connections are modelled as bonded contacts:

- Welded joints;
- The stepper and the gearhead together and with the stepper housing;
- The slip ring and the slip ring housing;
- The flywheel and the BLDC's shaft;
- The gimbal shaft and the gearhead's shaft;
- The sensor with the stepper housing cap and the offset gimbal bracket.

Two spherical joints modelled the bearings in the version with a slip ring. A revolute joint is set between the slip ring's rotor and the slip ring shaft.

The lower bearing's spherical joint is replaced with a revolute joint for the no slip ring version.

Generally, bolted links are not precisely modelled in FEA, but the CMG is a very small device, meaning that the manufactured parts are very stiff. Hence the deflections and induced stresses are low. On the other hand, small bolts might have non-negligible stress concentration. Four conditions are required to create a bolted joint. The contact between the bearing faces (bolts heads or nuts faces) and the surface of the part is set as a frictional contact with a friction coefficient of 0.6 (bolts and nuts being in steel and parts in aluminium—Table IV in [22]). The contact between the two, or more, bolted parts is defined as a frictional contact with a friction coefficient of one (aluminium on aluminium). Between the bolts, cylinders and the holes are defined frictional contacts with a 0.6 coefficient. These contacts model the threads' coefficient of friction. Usually, those contacts are lubricated and coefficient of friction lower. The shaft of the bolts is bounded to either the hole or the nut. Finally, *a bolt pretension* is applied on each bolt's rod. Two calculation steps must be defined, bolts are loaded in the first step and locked in the second. Assuming the clamp load (bolt pretension) is 80% of the yield load [23], the bolt designed preload is 723 N. Indeed, yield stress of a standard steel bolt is about 450 MPa, assuming the bolt's rod is a cylinder whose diameter is the bolt's nominal diameter, the yield load is 904 N.

As per the previous analysis, tetrahedron quadratic elements are defined on all parts. As the model has more parts than previously and to keep the computational need as low as possible, the global mesh size has been defined as 1 mm. Mesh is made smaller on thin parts in order to have at least two elements in the thickness. Therefore, a body sizing at 0.5 mm is applied on the flywheel motor mount, bolts, and nuts. The refinement function is used on the holes (threaded and through), making the mesh locally smaller, allowing a higher precision without increasing calculation time too much.

A coordinate system was created following the definition of the launcher's coordinate system detailed in the previous chapter. Quasi-static loads as defined in Table 3.2.1.1.a of Vega C user's manual [22] are used. The 4th event in this table corresponding to "*2nd stage ignition and flight, 3rd stage ignition*" has the biggest accelerations and is the acceleration applied on the previously created coordinate system.

Figure 7 shows the von Mises equivalent stress distribution in the CMG. The scale is deliberately exaggerated where every element with a stress above 50 MPa appears red. This is to emphasise the sparse stress distribution. As expected, stress is concentrated around the bolted areas. Three probes (A, B and C) are used to retrieve the maximum stress in the surface of two of the threaded holes in the stepper housing and a through hole in the flywheel motor mount. Excluding the vicinity of the holes, the stress due to the launch is negligible in the CMG.

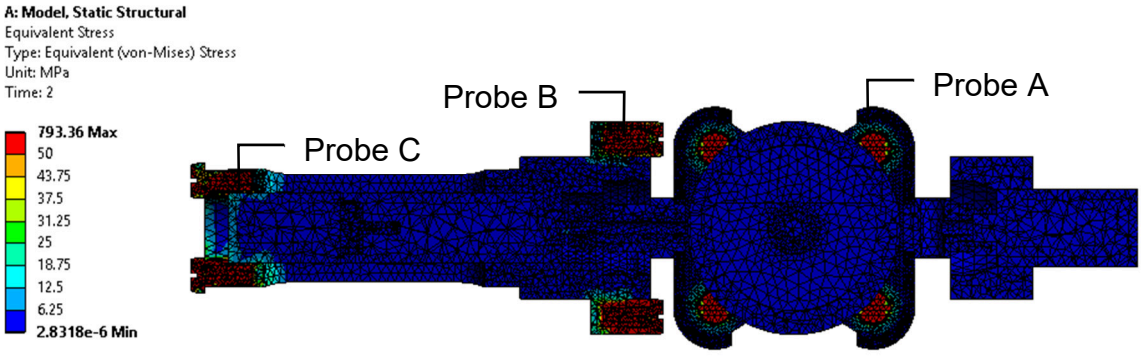

Figure 7. Distribution of von Mises equivalent stress [MPa] for the full CMG in static structural—Section view.

The maximum stress of these three probes is computed for different mesh size and plotted in Figure 8. Size of the elements of the flywheel motor mount is reduced from 0.5 to 0.3 mm with 0.05 mm increments, and the element size of the stepper housing is reduced from 1 to 0.6 mm with 0.1 mm increments. For the final value, the refinement value has been defined to three.

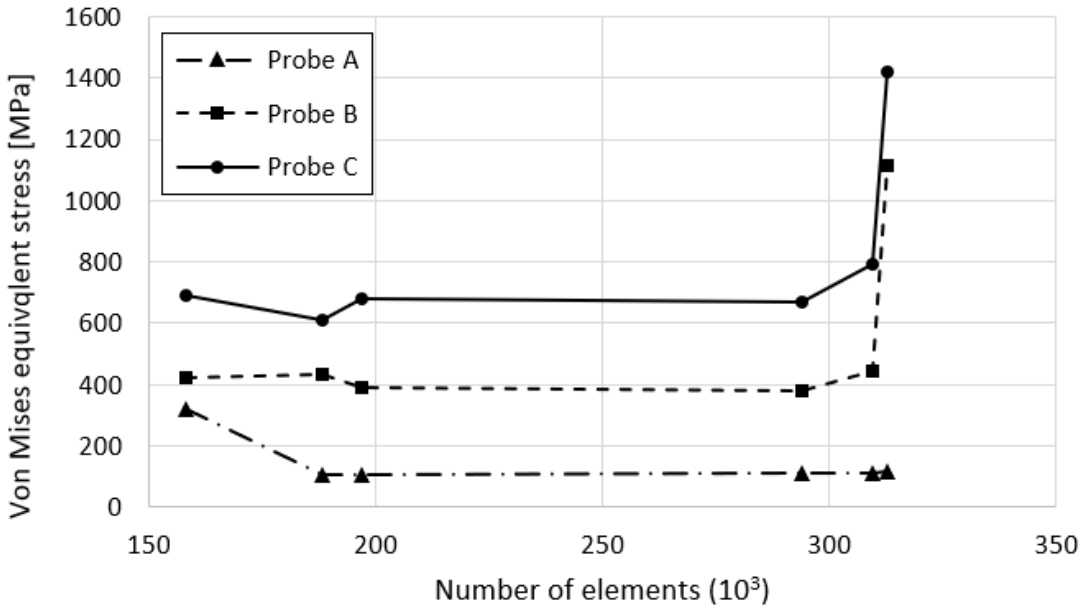

Figure 8. Maximum stress for Probes A, B and C in relation to the number of elements.

When reducing the mesh size and increasing the number of elements, the stress keeps increasing for Probes B and C. Divergence of the stress during mesh refinement is the sign of a singularity and is common around sharp edges or boundary conditions in this case. The theoretical value of the stress for Probes B and C is infinite, thus refining the mesh is only making the value closer to that theoretical value so increasing indefinitely. It is safe to ignore this value as it is only a consequence of the model and not a physical characteristic. On the other hand, Probe A is able to converge because

the problematic *bonded* contact condition is applied between the screw and the bolt, not the through hole. Indeed, St. Venant's principle states that local disturbances do not affect the stress distribution at sufficient distance. It would be safe to ignore that stress concentration if the stress in those local areas were not of interest. But bolted joints are critical, and the stress should be either analyzed with a more reliable simulation modelling the threads or via testing. The threaded holes are modelled as blind holes whose diameters are the nominal diameter of the holes. In reality, the tips of the threads in the real holes are closer to the surface of the part—the thickness of the material is even more reduced; hence, stress should be greater.

Locally increasing the thickness around the bolts is a possible solution. Indeed, although the stress at the singularity cannot be considered, a decent approximation is to measure the stress one element away from the singularity. Figure 9 shows that the stress quickly decreases away from the holes inner surface (where the bounded condition is applied, and the singularity occurs).

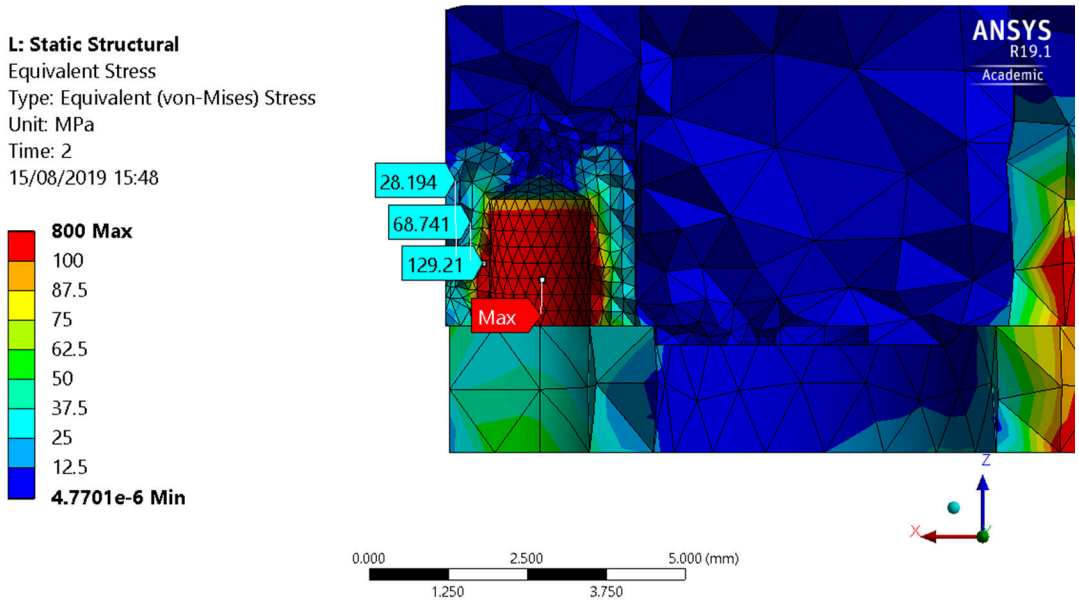

Figure 9. Stress some elements away from the singularity at Probe C—thickened version of the stepper housing, the external diameter of the stepper housing is increased at the bottom, the thickness increases from 2 to 4 mm.

If the stress at the bolted joint can be approximated by the stress one element away from the singularity (the inner surface of the hole), then the stress is below AA 6061-T6 yield stress (276 MPa). The bolted joints are the only critical features of the CMG as far as mechanical strength is concerned. Indeed, stress is not greater than 20 MPa away from those areas. Deformations are very small and do not exceed 0.015 mm. The greatest being at the tip of the stepper housing cap—the furthest from the fixed supports.

The modal analysis of the full CMG is not only a preliminary approach for the response spectrum analysis but also a way to confirm compliance with one of the launcher's requirements. Indeed, preventing coupling, the lowest natural frequencies of the spacecraft must be greater than those of the launcher. The CubeSat lowest natural frequencies should not be greater than those of the launcher if one of its subsystems (e.g., the CMG) have lower natural frequencies. It is therefore important to compute the CMG's natural frequencies. The analysis is performed on the pre-stressed model using the stress distribution from the previous structural analysis. The lowest natural frequency is 358.7 Hz which is way greater than the 12 Hz lateral and 20 Hz longitudinal natural frequencies of a Vega C [22]. For instance, on a non-pre-stressed CMG, the lowest natural frequency would be 529 Hz.

A response spectrum can then be performed for the CMG. Stresses induced by vibrations are especially important with beam- or plate-like components. Indeed, those shapes are more likely to have low natural frequency that with not much energy can be significantly deformed, deflections that are gradually increased by vibrations until potential failure. The shape and size of the CMG prevent such substantial deformations.

The results are based on the already converged mesh from the structural analysis; therefore, no additional mesh convergence is performed. The greatest stress is located in the gearhead shaft and evaluated at 2.3 MPa which is negligible. Indeed, as a result of the analysis of the flywheel assembly, the flywheel assembly's gimbal shaft is assumed bounded to the gear head shaft which does not rotate because of the stepper's holding torque. Although the modal analysis used the pre-stress from the static structural analysis, the stress distribution resulting from the response spectrum is not combined with the stress from static loads.

This analysis only reflects stress and deformations induced by vibrations. But mechanical failure of the material is not the only risk that a spacecraft faces during a launch. Although special fasteners are used to prevent them from loosening, this is not a risk one can ignore. Another consequence of vibrations is that it can separate electrical connections. In addition, it must be kept in mind that it may loosen any item such as adhesive or whiskers that can potentially, once in orbit, short-circuit electrical components or interfere with optical sensors or payload.

5. Discussion

Using CubeSats for missions that require agility has been made possible with the miniaturization of powerful and efficient miniature electric motors. Based on the requirements of an agile CubeSat, a 4-SGCMGs pyramidal configuration has been designed. Each SGCMG has a mass of about 35 g, and the total mass of the system is well below the 500g requirement and is estimated to 250g using avionics from existing ADCS systems currently in orbit. Compared to other CMG developments for CubeSats [6,12–19], the developed CMG can be a scalable solution for CubeSats of 1 to even 16U in size and the choice of a miniaturized stepper motor in a lean mechanical design brings a very lightweight design which can outperform reaction wheel systems in terms of mass, cost and performance. For example, similar reaction wheels with the same torque capability as the proposed CMG will weigh as much as the mechanical mass of the CMG cluster [4].

Electric motors (a BLDC motor for the flywheel and a stepper motor for the gimbal) have been chosen as the lightest of the market in terms of mass and are low cost components which can be built in space grade quality if necessary. Assuming a 0.2 rad/s gimbal rate, the angular momentum and thus the flywheel inertia has been computed to ensure a CubeSat up to 12U could perform a rotation of 90° in 90 s. The flywheel and other manufactured parts are designed to be lightweight and volume constrained. Two configurations of the CMG are possible, with and without a slip ring. The actual design of the CMG uses an inductive sensor for gimbal position initialization once in orbit. The motors selected also have significant margin in terms of performance (flywheel and gimbal speed), meaning that the torque and angular momentum of the system can be increased reasonably without changing any hardware. As cost was set as a requirement for the CMG, the motor and sensors cost for the proposed design where estimated to be less than 500 EUR sourced from European vendors such as Faulhaber.

Several FEA analyses have been performed to ensure and analyse the mechanical strength of the CMG against the launch environment. The preliminary analysis performed, as a first step, shows that the torque applied on the stepper motor's gearhead by the flywheel assembly during the launch would not exceed the stepper's holding torque, thus making the inductive sensor optional. Further analyses showed the maximum stress levels encountered by the manufactured part in static and sine responses. With the overall stress being very small, it has been decided to model the bolts pretention. This created singularities in the model but highlighted that those bolted joints are the critical parts of the CMG. In order to study them in more detail, a more detailed analysis requiring significant computational

time or testing is required. The sine response of the CMG in simulations indicated negligible stress, but the analysis performed did not consider the combination of a static and dynamic load. Shocks and random vibrations should also be studied to comply with the launcher's requirements.

Testing would also allow to measure effects of the vibrations that are not modelled in the presented FEA analyses, such as the loosening of bolts and the potential rupture of electronic connections. Apart from performing vibration studies, other tests should also be performed in the future. The dynamics of the CMG should be studied to ensure it does comply with the torque requirements and to precisely evaluate the power consumption of the electronic components. Performing operations of the CMG in a thermal vacuum chamber allows to study the effect of low temperatures and pression on the COTS motors. Furthermore, future testing with the manufactured hardware should take place to access the jitter, tolerances, and other dynamic behavior of the CMG.

6. Conclusions

In this paper, a novel, miniature, low-cost/-mass CMG actuator was conceptually designed for a range of CubeSat platforms with a size up to a 12U volume/mass and with a high agility requirement. The CMG designed uses miniature COTS motors and sensors, which are also low cost. It was shown that a 4-CMG cluster can fit in a 1U CubeSat and its mechanical mass without the avionics can be less than 150 g. A preliminary FEA analysis indicated that the CMGs using COTS components can survive launch loads and, thus, can be a feasible option for near-term CubeSat missions which require a high degree of maneuverability/slew capability compared to reaction wheel-based systems.

Author Contributions: A.G. performed the structural analysis and contributed on the design of the CMG and hardware selection. V.L. supervised the research work, research results and contributed in the CMG design, sizing, performance analysis and paper review/authorship. All authors have read and agreed to the published version of the manuscript.

Funding: This research received no external funding.

Conflicts of Interest: The authors declare no conflict of interest. The funders had no role in the design of the study; in the collection, analyses, or interpretation of data; in the writing of the manuscript, or in the decision to publish the results.

References

1. SpaceWorks. *Nano/Microsatellite Matket Forecast*, 9th ed.; SpaceWorks: Atlanta, GA, USA, 2019; Available online: https://www.spaceworks.aero/wp-content/uploads/Nano-Microsatellite-Market-Forecast-9th-Edition-2019.pdf (accessed on 12 May 2019).
2. European Space Agency. *ESA's 'CubeSat Central' for Smaller Missions into Space*; European Space Agency: Paris, France, 2019; Available online: https://www.esa.int/Our_Activities/Space_Engineering_Technology/ESA_s_CubeSat_central_for_smaller_missions_into_space (accessed on 12 May 2019).
3. Steyn, W.H.; Lappas, V. *Chapter I-2c: Attitude Control and Determination, Nanosatellites: Space and Ground Technologies, Operations and Economics*; de Carvalho, R.A., Estela, J., Langer, M., Eds.; Wiley: Hoboken, NJ, USA, March 2002. [CrossRef]
4. Lappas, V. 'QB50 ADCS and GPS Subsystem', 3rd QB50 Workshop, Belgium. 2012. Available online: https://www.qb50.eu/download/3rdQB50Workshop_presentations/07-ADCS%202.2.12-Lappas-3rdQB50Workshop.pdf (accessed on 15 April 2020).
5. Bridges, C.P.; Kenyon, S.; Shaw, P.; Simons, E.; Visagie, L.; Theodorou, T.; Yeomans, B.; Parsons, J.; Lappas, V.; Underwood, C. A Baptism of Fire: The STRaND-1 Nanosatellite. In Proceedings of the 27th AIAA/USU Conference, Small Satellite Constellations, Logan, UT, USA, 10–15 August 2013; paper: SSC13-X-3. Available online: https://pdfs.semanticscholar.org/e58b/80cf5653a03ead2929b358be91a9000bfe3b.pdf (accessed on 15 April 2020).
6. Lappas, V.J. *CMG Based AOCS for Agile Small Satellite*; University of Surrey: Guildford, UK, 2002; Available online: https://core.ac.uk/display/101476 (accessed on 15 May 2019).
7. Wie, B. *Space Vehicle Dynamics and Control, 2nd ed*; American Institute of Aeronautics and Astronautics: Phoenix, AZ, USA, 2012. [CrossRef]

8. Heiberg, C.J.; Bailey, D.; Wie, B. Precision Spacecraft Pointing Using Single-Gimbal Control Moment Gyroscopes with Disturbance. *J. Guid. Control Dyn.* **2008**, *23*, 77–85. [CrossRef]
9. Defendini, A.; Morand, J.; Faucheux, P.; Guay, P.; Rabejac, C.; Bangert, K.; Heimerl, H. Control Moment Gyroscope (CMG) Solutions for Small Satellites. In Proceedings of the 28th Annual AAS Rocky Mountain Guidance and Control Conference, Breckenridge, CO, USA, 5–9 February 2005; AAS 05-004.
10. Leve, F.A.; Hamilton, B.J.; Peck, M.A. Introduction. In *Spacecraft Momentum Control Systems*; Space Technology Library, Springer: Cham, Switzerland, 2015; Volume 1010.
11. Lappas, V.; Oosthuizen, P.; Madle, P.; Cowie, L.; Yuksel, G.; Fertin, D. Micro CMGs for Agile Small Satellites Design and In-orbit Tests. In Proceedings of the 6th International ESA Conference on Guidance, Navigation and Control Systems, Loutraki, Greece, 17–20 October 2005. (ESA SP-606, January 2006)
12. Lappas, V.; Steyn, W.H.; Underwood, C. Design and testing of a control moment gyroscope cluster for small satellites. *J. Spacecr. Rocket.* **2005**, *42*, 729–739. [CrossRef]
13. Votel, R.; Sinclair, D. Comparison of Control Moment Gyros and Reaction Wheels for Small Earth-Observing. In Proceedings of the 26th Annual AIAA/USU Conference on Small Satellites, Logan, UT, USA, 13–16 August 2012; pp. 1–7.
14. Chang, H.; Jiao, W.; Fu, Q.; Xie, J.; Yuan, W. Design and Simulation of a MEMS Control Moment Gyroscope for the Sub-Kilogram Spacecraft. *Sensors* **2010**, *10*, 4130–4144. [CrossRef] [PubMed]
15. Patankar, K.; Fitz-Coy, N.; Roithmayr, C.M. Design Considerations for Miniaturized Control Moment Gyroscopes for Rapid Retargeting and Precision Pointing of Small Sat. In Proceedings of the Utah Small Satellite Conference, Logan, UT, USA, 7 July 2014. SSC14-III-8.
16. Nagabhushan, V. Development of Control Moment Gyroscopes for Attitude Control of Small Satellites. Master's Thesis, University of Florida, Gainesville, FL, USA, 2009.
17. Honeybee Robotics. Microsat CMG Attitude Control Array. 2019. Available online: https://www.honeybeerobotics.com/wp-content/uploads/2014/03/Honeybee-Robotics-Microsat-CMGs.pdf (accessed on 8 May 2019).
18. Akiyama, K.; Fujihashi, K.; Matunaga, S. High-Speed Attitude Control System for Small Satellite with Micro-CMGs. *Trans. Jpn. Soc. Aeronaut. Space Sci. Aerosp. Technol. Jpn.* **2012**, *8*, Pd_91–Pd_97. [CrossRef]
19. Baker, N. Feasibility and Design of Miniaturized Control Moment Gyroscope for a 3-Axis Stabilized Micro Satellite. Master's Thesis, Lulea University of Technology, Luleå, Sweden, 2016. Available online: https://www.diva-portal.org/smash/get/diva2:1053012/FULLTEXT01.pdf (accessed on 12 May 2019).
20. Wertz, J.R.; Everett, D.F.; Puschell, J. *Space Mission Engineering: The New SMAD*, 5th ed.; Microcosm Press: Portland, OR, USA, 2011.
21. Hevner, R.; Holemans, W.; Puig-Suari, J.; Twiggs, R. An Advanced Standard for CubeSats Conference on Small Satellites. In Proceedings of the 25th Annual AIAA/USU Conference on Small Satellites, Logan, UT, USA, 8–11 August 2011; pp. 1–12. Available online: http://digitalcommons.usu.edu/cgi/viewcontent.cgi?article=1111&context=smallsat (accessed on 21 May 2019).
22. Arianespace. *Vega C User's Manual*; Arianespace: Courcurona, France, 2018; Available online: http://www.arianespace.com/wp-content/uploads/2018/07/Vega-C-user-manual-Issue-0-Revision-0_20180705.pdf (accessed on 7 August 2019).
23. Shoberg, R.S. *Engineering Fundamentals of Threaded Fastener Design and Analysis*; RS Technologies: Farmington Hills, MI, USA, 2000; Available online: http://www.hexagon.de/rs/engineering.fundamentals.pdf (accessed on 9 August 2019).

© 2020 by the authors. Licensee MDPI, Basel, Switzerland. This article is an open access article distributed under the terms and conditions of the Creative Commons Attribution (CC BY) license (http://creativecommons.org/licenses/by/4.0/).